An entropy regularization method applied to the identification of wave distribution function for an ELF hiss event

Olivier Prot,[1,2] Ondřej Santolík,[3,4] Jean-Gabriel Trotignon,[5] and Hervé Deferaudy[6]

Received 5 January 2005; revised 5 November 2005; accepted 17 January 2006; published 22 June 2006.

[1] An entropy regularization algorithm (ERA) has been developed to compute the wave-energy density from electromagnetic field measurements. It is based on the wave distribution function (WDF) concept. To assess its suitability and efficiency, the algorithm is applied to experimental data that has already been analyzed using other inversion techniques. The FREJA satellite data that is used consists of six spectral matrices corresponding to six time-frequency points of an ELF hiss-event spectrogram. The WDF analysis is performed on these six points and the results are compared with those obtained previously. A statistical stability analysis confirms the stability of the solutions. The WDF computation is fast and without any prespecified parameters. The regularization parameter has been chosen in accordance with the Morozov's discrepancy principle. The Generalized Cross Validation and L-curve criterions are then tentatively used to provide a fully data-driven method. However, these criterions fail to determine a suitable value of the regularization parameter. Although the entropy regularization leads to solutions that agree fairly well with those already published, some differences are observed, and these are discussed in detail. The main advantage of the ERA is to return the WDF that exhibits the largest entropy and to avoid the use of a priori models, which sometimes seem to be more accurate but without any justification.

Citation: Prot, O., O. Santolík, J.-G. Trotignon, and H. Deferaudy (2006), An entropy regularization method applied to the identification of wave distribution function for an ELF hiss event, *J. Geophys. Res.*, *111*, A06213, doi:10.1029/2005JA011006.

1. Introduction

[2] The propagation direction of an electromagnetic wave in a homogeneous medium can be modeled by the wave distribution function (WDF). The concept of WDF was introduced by *Storey and Lefeuvre* [1974, 1979, 1980] to study the propagation of electromagnetic waves in plasma. It is a positive function which represents the directional distribution of the electromagnetic wave energy. The WDF $F(\theta, \phi)$ is related to the estimated spectral matrix components V_{ij} by the integral equation over the unit sphere $[0, \pi] \times [0, 2\pi]$:

$$V_{ij} = \int_0^{\pi} \int_0^{2\pi} Q_{ij}(\theta, \phi) F(\theta, \phi) \sin\theta \mathrm{d}\phi \mathrm{d}\theta, \qquad (1)$$

where Q_{ij}:$[0, \pi] \times [0,2\ \pi] \rightarrow C$ are the integration kernels. They correspond to the auto- and cross-power spectra of the electromagnetic components of a plane wave in a given polarization mode [*Lefeuvre and Pinçon*, 1992]. The kernels Q_{ij} are known analytical functions that depend on the ambient plasma parameters. Their algebraic expressions in the cold plasma case are given by *Storey and Lefeuvre* [1980]. The angles θ and ϕ are defined in Figure 1.

[3] We want to compute the WDF from the spectral matrix V through equation (1). This is clearly an ill-posed inverse problem; hence we must make further assumptions on F to get a stable solution. There are many methods to solve this kind of inverse problem, for example the method of maximum entropy (ME) of *Lefeuvre and Delannoy* [1979, 1986] in the cold plasma case. This method was modified by *Santolík* [1995] and *Santolík and Parrot* [1996] for a hot plasma, including Doppler effect. Another way to solve this inversion problem is to choose a parametric model for the WDF and then to identify the parameters that best fit the data. This identification is often made using a least-square minimization, for example, in the Levenberg-Marquardt algorithm [*Press et al.*, 1986; *Bergounioux*, 2002]. With this approach, *Santolík and Parrot* [2000] used a Gaussian peaks (GP) model to solve equation (1). Nevertheless, some problems arise because several parameters of the WDF models have to be fixed before starting computations. As a consequence, numerous solutions are

[1]MAPMO, Université d'Orléans, France.
[2]Also at Laboratoire de Physique et Chimie de l'Environnement, Centre National de la Recherche Scientifique, Orléans, France.
[3]Faculty of Mathematics and Physics, Charles University, Prague, Czech Republic.
[4]Also at Institute of Atmospheric Physics, Academy of Sciences of the Czech Republic, Prague, Czech Republic.
[5]Laboratoire de Physique et Chimie de l'Environnement, Centre National de la Recherche Scientifique, Orléans, France.
[6]Centre d'Étude des Environnements Terrestre et Planétaires, Institut Pierre Simon Laplace, Vélizy, France.

0148-0227/06/2005JA011006

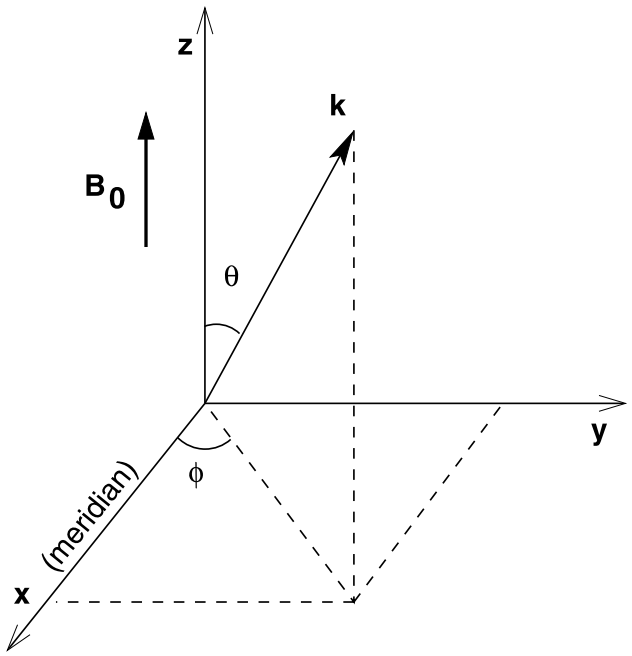

Figure 1. The polar θ and azimuthal ϕ angles in the spacecraft coordinate system.

obtained and there is no way to determine which one is the best.

[4] The key step of *Lefeuvre and Delannoy* [1986] maximum entropy method is to orthogonalize the kernels Q_{ij} and then to make a truncation in order to retain the dominant linearly independent kernels. The discarded kernels are assumed unimportant for the wave analysis due to their low eigenvalues. In this process, many components of the initial spectral matrix are unfortunately lost.

[5] In this paper, we use a new algorithm, called ERA (entropy regularization algorithm), which is based on the concept of entropy minimization to find the propagation direction of an electromagnetic wave. This method was developed by *Prot et al.* [2005] for the case of a linear inverse problem with finite dimensional data and a positivity constraint. The algorithm is easy to use, the computations are fast, and the resulting solutions minimize the entropy in the probabilistic sense. Therefore it partially fixes the nonlinear dependence of the solution introduced by entropic inversion methods. *Prot et al.* [2005] tested the ERA in the case of waves propagating in vacuum. Satisfactory results have been obtained for simulated noisy spectral matrices. The ability of the ERA technique to detect a single plane-wave has also been studied in the case of a cold plasma model [*Prot et al.*, 2004].

[6] Regularization methods are widely used to solve ill-posed problems [*Tikhonov and Arsenin*, 1977; *Kirsch*, 1996]. The WDF obtained by using entropy as the regularizing functional represents the minimum information required to fit/explain the data [*Shore and Johnson*, 1980; *Oscarsson*, 1994]. To ensure the stability of the solution, a regularization parameter has to be fixed, and, unlike in the ME method, no data of the spectral matrix needs to be rejected. In our computation, the regularization parameter is automatically selected in accordance with the Morozov's discrepancy principle [*Kirsch*, 1996].

[7] The objective of the paper is to show the results obtained with the entropy regularization method, ERA, applied for the first time to experimental data. The ERA method, as well as the maximum entropy (ME) and Gaussian peaks (GP) methods are recalled in section 2, for comparison. Section 3 starts with a brief description of the FREJA magnetospheric mission which provided the data used here. Then, a description of the ERA algorithm is presented at the end of section 3. Finally, before the discussions and conclusions, the FREJA data-analysis results are presented in section 4. In particular, the stability of the resulting ERA solutions is statistically evaluated.

2. Methods

2.1. Description of Two Other WDF Methods

[8] The methods for computing the WDF considered here [*Santolík*, 1995; *Santolík and Parrot*, 2000] are based on least squares fit techniques. As parametric models of the WDF are used, the problem amounts to determining the parameter values that best fit the data.

[9] In his thesis, *Santolík* [1995] used a model of Gaussian peaks (GP) to compute the WDF. The main advantage of the GP is that it returns the best solution when the number of peaks, i.e., the number of wave propagation directions is known in advance. For each peak, the energy, the beam width, and the angles (θ, ϕ) that describe the propagation direction are computed. It is worth noting that with many (>3) peaks, the obtained solution becomes unstable, and sometimes no solution at all is found. As the expected number of peaks is usually unknown, the GP can not be used automatically in statistical analysis.

[10] In the Lefeuvre and Delannoy method (ME) [*Lefeuvre*, 1977; *Lefeuvre and Delannoy*, 1979, 1986] the model for the WDF is chosen to maximize the entropy. The only parameters to compute are the Lagrange multipliers of the maximization problem. However, since the integration kernels are not linearly independent, they have to be orthogonalized, and thus many dependent kernels have to be discarded to obtain a stable solution. In this process, it is assumed that the discarded kernels are insignificant for the wave analysis. In practice, the number of discarded kernels is fixed before the computation, and the geometry of the solution turns out to depend on it. *Storey* [1987] has shown that some spectral matrices cannot be analyzed with this method because the discarding process leads to WDF solutions that do not fit the measured spectral matrix. This limitation has encouraged us to use a regularization technique that allows the whole initial spectral matrix to be kept, with the solution regularized for stability.

[11] In the literature, the GP and ME methods have not been used automatically, mainly because some parameters have to be fixed before starting the computation. The ERA method presented here should, in principle, be well-suited for this kind of analysis. The details of GP and ME methods are described by *Lefeuvre and Delannoy* [1986], *Santolík* [1995], and *Santolík and Parrot* [2000]. We can also mention the method of *Oscarsson et al.* [2001], where an alternative form for the WDF is used and is not comparable with the one proposed here. The entropy regularization

method presented here starts from a different point of view. The main advantage of this point of view is that we do not have to choose any model for the WDF or use a least squares minimization. The solution is computed by solving an optimization problem via an iterative algorithm.

2.2. Entropy Regularization

[12] The regularization theory, used to solve ill-posed problems, is based on the use of a family of operators indexed by a free positive parameter μ. When μ is small, the error in the solution is small but the solution becomes strongly unstable. Conversely, the error increases with larger μ but the stability is assured. So, a compromise between error and stability must be found. A most often used method of regularization is the one of Tikhonov [*Tikhonov and Arsenin*, 1977; *Tikhonov et al.*, 1995]. For the sake of simplicity, the spectral matrix V and the integration kernels are identified as a vector in $\mathbb{C}^n$ and a function Q: $[0, \pi] \times [0, 2\pi] \rightarrow \mathbb{C}^n$, respectively. Tikhonov's regularization principle is to solve

$$\min_F \varepsilon_r(V,F) + \mu\|F\|^2 \ , \ F \geq 0, \tag{2}$$

where $\mu > 0$ is the regularization parameter and $\varepsilon_r(V, F)$ is the error in the data

$$\varepsilon_r(V,F) := \left\| V - \int_0^{\pi}\int_0^{2\pi} Q(\theta,\phi)F(\theta,\phi)\sin\theta \mathrm{d}\phi\mathrm{d}\theta \right\|^2_{\mathbb{C}^n}.$$

The strict convexity of the functional norm $\|F\|^2 := \int_0^{\pi}\int_0^{2\pi} |F(\theta, \phi)|^2 \sin\theta \mathrm{d}\phi\mathrm{d}\theta$ will ensure the stability of the solution. Unfortunately, it does not guarantee that the resulting WDF is positive; therefore it cannot be used for our purpose.

[13] The entropy regularization principle is quite similar, but here the entropy, instead of the norm, is used as a regularizing functional. The entropy is based on the concept of the relative information content. *Shore and Johnson* [1980] have shown that for two probability densities f and g, the information content $I(f, g)$ of f relative to g can be quantified by

$$I(f,g) := \int_0^{\pi}\int_0^{2\pi} f(\theta,\phi)\ln\frac{f(\theta,\phi)}{g(\theta,\phi)}\sin\theta \mathrm{d}\phi\mathrm{d}\theta. \tag{3}$$

The entropy of a probability density is then defined by $-H := -I(f, \bar{g})$, where $\bar{g}$ is the noninformative probability density, i.e., $\bar{g}$ is the density of the noise in the physical system. Since isotropy is assumed for the determination of the wave-energy density, $\bar{g}$ is assumed to be constant. Hence the entropy is defined by

$$-H(F) := -\int_0^{\pi}\int_0^{2\pi} F(\theta,\phi)\ln F(\theta,\phi)\mathrm{d}\phi\mathrm{d}\theta \tag{4}$$

Using H as a regularizing functional has advantages; it leads to a smooth and positive solution, which is well suited in our framework. Moreover, the minimization of H flattens the solution. In fact, when $\mu \rightarrow +\infty$ the resulting solution becomes constant, which means that we have only trivial information about the variations in the wave-energy density.

[14] The use of the entropy to solve an ill-posed problem is now a standard method in image restoration [*Press et al.*, 1986], radio astronomy, seismology, and many other applications [*Smith and Grandy*, 1987]. According to *Oscarsson* [1994], the minimization of entropy functional can be used in the WDF computation to reproduce the structures required by the data in the wave-energy density, with suppressed spurious peaks. Thus we need to solve

$$\min_F \varepsilon_r(V,F) + \mu H(F) \ , \ F \geq 0. \tag{5}$$

This optimization problem has a unique solution for all μ [*Amato and Hughes*, 1991], denoted by F_μ. *Amato and Hughes* [1991] and *Engl and Landl* [1993] have shown the convergence of F_μ to the solution of maximum entropy, as $\mu \rightarrow 0$. In our case, to ensure the stability of solution, the regularization parameter μ cannot be chosen too small. A fixed-point algorithm has been investigated by *Prot et al.* [2005] to solve (5) for large μ. This algorithm leads to a smooth solution.

[15] As already stated, the regularization parameter $\mu > 0$ must be chosen sufficiently small to get a low error $\varepsilon_r(V, F_\mu)$, but it should be chosen large enough for the stability of the solution F_μ. The method used to choose μ will be described in subsection 2.3.

[16] In fact, $-H$ is not the entropy in the probabilistic sense since the WDF F is not a probability density on $[0, \pi] \times [0, 2\pi]$. This implies that the solution F_μ is not linearly dependent on the data V. Indeed, for the spectral matrix $V' = \lambda V$, the solution of (5) is not λF_μ. This is very annoying since the data are always scaled for numerical computations. That is why we have modified the optimization problem to minimize the entropy in the probabilistic sense. Thus the new optimization problem becomes

$$\begin{cases} \min_{(\alpha,f)} \varepsilon_r(V, \alpha f) + \mu H(f) \\ f \gtrsim 0, \int_0^{\pi}\int_0^{2\pi} f(\theta,\phi)\mathrm{d}\phi\mathrm{d}\theta = 1, \alpha > 0. \end{cases} \tag{6}$$

In this problem α represents the power of the electromagnetic wave and f the probability distribution of the wave direction. The function f is a probability density because of the integral constraint. From this point of view, the WDF of the wave is actually $F = \alpha f$.

[17] The minimization problem (6) is much more difficult to solve than (5). We do not have a guaranteed optimality condition for this problem since the cost function is not convex and the solution may not be unique. Nevertheless, *Prot et al.* [2005] have established an iterative algorithm to compute a local solution of (6). This entropy regularization algorithm is as follows.

[18] 1. Initialization. Choose $V \in \mathbb{C}^n$, $l_0 \in \mathbb{C}^n$, $\mu > 0$, $\epsilon > 0$, $\tau \in]0, 1]$.

[19] 2. Iteration κ. First, compute

$$g(l_{\kappa-1}) := \int_0^{\pi}\int_0^{2\pi} Q(\theta,\phi)\Gamma(l_{\kappa-1})(\theta,\phi)\mathrm{d}\phi\mathrm{d}\theta$$

where $\Gamma(l_{\kappa-1}) := \exp\left(-1 + \frac{2}{\mu}\psi^*[l_{\kappa-1}]\ (\theta, \phi)\ \right)$ and $\psi^*[l](\theta, \phi) := \sum_{j=1}^n l_j Q_j\ (\theta, \phi)$. Then, compute $\delta_{\kappa-1} := \frac{Re\langle V g(l_{\kappa-1})_{\mathbb{C}^n}\rangle}{\langle g(l_{\kappa-1}) g(l_{\kappa-1})_{\mathbb{C}^n}\rangle}$. Then, $l_\kappa = (1 - \tau)l_{\kappa-1} + \tau(V - \delta_{\kappa-1}g(l_{\kappa-1}))$.

[20] 3. Stopping criterion. If $|l_\kappa - l_{\kappa-1}| < \epsilon$, then STOP, else $\kappa := \kappa + 1$ and go to 2.

[21] Suppose that $\alpha_\kappa \to \alpha$ and $l_\kappa \to l$ then (α^*, F^*) is a local solution of (6) [*Prot et al.*, 2005], where

$$\alpha^* = \frac{\alpha}{\int_S \Gamma(l)\mathrm{d}\sigma}$$

and

$$F^* = \frac{\Gamma(l)}{\int_S \Gamma(l)\mathrm{d}\sigma}.$$

The convergence of this algorithm has been proved when the regularization parameter is chosen large enough [*Prot et al.*, 2005]. However, we do not know whether it converges for every values of $\mu > 0$, but it does work well numerically. We need a small parameter τ for the convergence of the algorithm, but it should not be too small to ensure fast computations. The choice of τ does not affect the solution but small values slow down the computation. In our algorithm, the parameter τ is computed automatically by the following rule: if ERA diverges, i.e., if $\|l_{\kappa+1} - l_\kappa\| > \|l_\kappa - l_{\kappa-1}\|$, we let $\tau_{n+1} = r\tau_n$ where $0 < r < 1$ and then restart the computation until it converges. After this, to refine the value of τ, we use a linear search, choosing the largest parameter $\{[(N - k)r\tau + k\tau]/N;\ k = 0, \ldots, N - 1\}$ for which ERA continues to converge.

[22] We must now check if the nonlinearity problem introduced by the entropy is actually solved. By taking the data $V' = \lambda V$ for $\lambda > 0$, we see from the minimization problem (6) that the corresponding solution is nothing but ($\lambda\alpha^*$, F^*) for the regularization parameter $\mu\lambda^2$. *Prot et al.* [2005] have shown that this remains true for the local solution computed by the ERA. In the next section, this algorithm will be used to compute the WDF using the measurements from the FREJA satellite. However, a rule to find an appropriate regularization parameter has to be defined.

2.3. Choice of the Regularization Parameter

[23] The choice of the regularization parameter is an intricate problem, since we must trade off between the error and stability of the solution. For the stability of the solution, μ must not be too small, whereas for a small error of fit this parameter must not be too large. In our computation, the Morozov's discrepancy principle will be used to automatically choose this parameter. Essentially, solutions whose errors of fit are smaller than the measured noise level cannot in any way be considered as valid.

[24] Let $\mu > 0$ and denote by (α_μ, F_μ) the obtained solution of (6). Suppose that the noise level in the data is $\delta > 0$, then choose the regularization parameter $\mu > 0$ such that $\varepsilon_r(V, F_\mu) = \delta$. However, numerically, an equality is too restrictive. A μ that satisfies $\varepsilon_r(V, F_\mu) \geq \delta \pm 10\%$ is acceptable. To find such a μ, we use the fact that $\mu \to \varepsilon_r(V, F_\mu)$ is quite linear for small μ. More precisely, our rule will be (1) choose $\mu_0 > 0$, (2) compute F_{μ_k}, (3) if $\varepsilon_r(V, F_{\mu_k}) = \delta \pm 10\%$ STOP, else

$$\mu_{k+1} = \varepsilon_r\left(V, F_{\mu_k}\right)\frac{\delta}{\mu_k}$$

and go to 1.

[25] In fact, δ is not exactly the noise level; it is the estimation of the statistical error in the spectrum values. The number δ is computed when the estimation of the spectral matrix is done.

2.4. Stability Analysis

[26] In subsection 2.3 we have described how the regularization parameter μ in the algorithm is determined. In fact, μ is chosen such that the error in the data is equal to δ $\pm 10\%$. We know that for all $\mu > 0$ the solution varies continuously as a function of the data, but a small perturbation of the spectral matrix could lead to a huge modification of the solution. To verify and quantify this, some statistical tests have to be done.

[27] For this purpose, perturbed spectral matrix $V_N := V + N$ must be created, where V is the measured spectral matrix, N is the perturbation matrix ($N = bb^*$), with b a random Gaussian vector. Then the energy perturbation, C_1, and the variation for each points of the perturbed solution, C_∞:[0, π] $\times$ [0, 2π] $\to R^+$, can be computed from the perturbed solution F_N. C_1 and C_∞ are given by

$$C_1 := \frac{\int_0^\pi \int_0^{2\pi} |F(\theta,\phi) - F_N(\theta,\phi)| \sin\theta \mathrm{d}\phi\mathrm{d}\theta}{\| V - V_N \|}, \tag{7}$$

$$C_\infty(\theta,\phi) := \frac{|F(\theta,\phi) - F_N(\theta,\phi)|}{\| V - V_N \|}. \tag{8}$$

The process is then repeated for a large number of random Gaussian vectors b. From the C_1 sample thus obtained, the expectation, the variance, and the quantity $V_1(\delta)$ that represents the relative power error of the perturbed solution are computed. $V_1(\delta)$ is defined as

$$V_1(\delta) := \frac{E(C_1)\sqrt{\delta}}{\int_0^\pi \int_0^{2\pi} |F(\theta,\phi)| \sin\theta \mathrm{d}\phi\mathrm{d}\theta}, \tag{9}$$

and expressed in percent. In addition, from the expectation of the C_∞ sample, a map of the averaged variation of the perturbed WDF can be plotted on the sphere [0, π] $\times$ [0, 2π].

[28] In the work of *Lefeuvre and Delannoy* [1986], the stability of the solution is expressed in terms of the ratio of the mean-square error in the solution to the mean-square value of the solution itself. Instead of this stability parameter, we have chosen to use C_1. The main reason for this choice is that C_1 has the dimension of an energy, while the stability parameter in the work of *Lefeuvre and Delannoy* [1986] is related to the square of the energy, which is less convenient. The number C_1 and the function C_∞: [0, π] $\times$ [0, 2π] $\to R^+$ allow the stability of the solution, namely the WDF, to be quantified from two opposite points of view. Unlike C_1, which is a global estimator of the stability, the function C_∞ indeed measures the local deviation of the perturbed WDF compared with the nonperturbed solution. It is noteworthy that it becomes possible to highlight the place where the solution is the most unstable from the expectation of C_∞, as we will see in section 4.2.

[29] An important point is actually to clarify the stability of the solutions as a function of the regularization parameter

μ. To do so, the solutions F_μ can be computed for a sufficient number of μ values (100) in $[\mu_d, \mu_u]$ with $0 < \mu_d < \mu_u$. Then, the stability index

$$S(\mu) := \sqrt{\frac{\int_0^{\pi}\int_0^{2\pi}\left|F_\mu(\theta,\phi) - F^*(\theta,\phi)\right|^2 \sin\theta \mathrm{d}\phi\mathrm{d}\theta}{\int_0^{\pi}\int_0^{2\pi}\left|F^*(\theta,\phi)\right|^2 \sin\theta \mathrm{d}\phi\mathrm{d}\theta}}. \quad (10)$$

can be computed. The optimal solution in the Morozov sense F^* is numerically defined by $F^* = F_{\mu^*}$, with

$$\left(\delta - \varepsilon_r\left(V, F_{\mu_*}\right)\right)^2 = \min_{\mu\in[\mu_d,\mu_u]}\left(\delta - \varepsilon_r\left(V, F_\mu\right)\right)^2.$$

The stability index S allow us to quantify the variation of F_μ with respect to F^*, it is also insensitive to the scale of the optimal solution F^* due to the normalization.

3. ERA Implementation on the FREJA Data

[30] FREJA is a low-altitude magnetospheric research satellite. The F4 onboard wave experiment [*Holback et al.*, 1994] measured waveforms of three orthogonal magnetic components and one electric component received by a spinning antenna. The F4 experiment has observed an intense emission of ELF hiss on 8 April 1995, between 1548 and 1558 UT. *Santolík and Parrot* [2000] have made a plane-wave analysis of this event and a WDF analysis on six different points of the ELF hiss spectrogram.

[31] For our WDF analysis we use the same data as *Santolík and Parrot* [2000]; that is, the six spectral matrices and the six error matrices corresponding to the six points in the spectrogram. Since FREJA measured three magnetic and one electric components, the spectral and the error matrices are 4×4. These matrices are identified as vectors in $\mathbb{C}^{16}$ and denoted by $v^k \in \mathbb{C}^{16}$ for the spectral matrices and by $e^k \in \mathbb{C}^{16}$ for the measurement-error matrices for points $k = 1, \ldots, 6$. The measurement-error matrix is needed since we do not have the same quality of measurement on each of the antennae. The error matrix is computed using the statistical standard deviation of the spectral values.

[32] We also use the same integration kernels as in the work of *Santolík and Parrot* [2000]. These kernels have been computed according to a assumed plasma model. They use the cold plasma approximation with the hypothesis of a collisionless, singly ionized oxygen-hydrogen plasma with 5% fraction for the hydrogen. The composition of the plasma is rather important, since the frequency of the waves is lower than $2f_{H^+}$, where f_{H^+} is the proton gyrofrequency. The right-hand polarization mode has been used to compute these kernels for frequencies above f_{H^+} because this mode is the only one expected in a cold plasma at these frequencies [*Styx*, 1992]. We denote by $q^k{:}S \to \mathbb{C}^{16}$ the computed integration kernels corresponding to points $k = 1, \ldots, 6$.

[33] To take into account the measurement-error matrix, the data and the integration kernels are normalized. More precisely, for all $i = 1, \ldots, 16$, we let

$$V^k = \begin{pmatrix} v_i^k \\ \overline{e_i^k} \end{pmatrix} \in \mathbb{C}^{16} \quad \text{and} \quad \bar{Q}_k = \begin{pmatrix} q_i^k \\ \overline{e_i^k} \end{pmatrix}$$

be the normalized spectral matrix and the normalized integration kernel. The goal of this normalization is to have the same order of error in each of the spectral matrix components. As a consequence, the noise level of the normalized data becomes $\delta = 16$.

[34] As the kernel values often vary over a large range, for good computational performance it is necessary to scale them by letting $Q^k = 10^{-\beta}\,\bar{Q}^k$ such that $1 \le \max|Q_i^k| \le 50$ for all $i = 1, \ldots, 16$. The β values for each of the six points are given in Table 1.

[35] The FREJA F4 data is first transformed into the same coordinate system as used in the work of *Santolík and Parrot* [2000]; the z axis is parallel to the Earth magnetic field, and the x axis points toward the direction of decreasing magnetic latitude in the magnetic meridian plane (see Figure 1). The k wave-normal direction is determined by the angles θ (polar) and ϕ (azimuthal).

4. FREJA Data Analysis Results

[36] As mentioned before, the ERA algorithm has been applied to the same six time-frequency points as in the work of *Santolík and Parrot* [2000]. The same graphical representation is also used, for easy comparison. An example of this is given in Figure 2, which is a spherical plot of the WDF value as a function of $0 \le \theta \le \pi$ and $0 \le \phi \le 2\pi$. In the northern hemisphere (left plot) θ varies from 0 to $\pi/2$, while in the southern one (right plot) it runs over $[\pi/2, \pi]$.

[37] In our computations, the parameter ϵ used in the stopping criterion and the first step of the algorithm are set at $1e-7$ and 0. All the computation have been made with the scientific software MATLAB® on an Apple ibook G3 700 MHz. The computation times are variable depending on the integration kernel, the data, and the algorithm parameters. Generally, computations are quite fast and the solutions are obtained in a few seconds. For example, the stability computations described in the previous section took approximately 1 hour for 1000 computed solutions.

4.1. Computed WDF

[38] In Figure 3 are displayed the WDFs for each of the six FREJA time-frequency points, computed using the following three methods (from top to bottom): the entropy regularization algorithm (ERA), the Gaussian peaks method (GP), and the maximum entropy technique (ME). The level contours around the WDF peak are superimposed and are shown as dashed lines in the ERA plots and as solid lines in the GP and ME plots.

[39] On the whole, the ERA solutions turn out to be more spread out than both the ME and GP solutions; nevertheless, there are no large discrepancies among all these solutions. If we now look at the various solutions in greater detail, there are actually some significant differences.

[40] For the first point, the plane wave analysis made by *Santolík and Parrot* [2000] returns a downgoing wave at $\theta \approx 30°$, $\phi \approx 45°$ with a high degree of polarization. As shown in the top left panel of Figure 3, the GP and ME solutions exhibit a sharp peak in almost the same position, which is also in fairly good agreement with the position obtained by the plane-wave analysis. If we now look at the ERA solution, it becomes clear that the main peak occurs at the right place ($\theta \approx 14°$, $\phi \approx 43°$) in the northern

Table 1. Results Obtained for Each Point[a]

Point	1	2	3	4	5	6
Time, UT	1549:15	1552:43	1552:43	1554:59	1554:59	1555:53
Frequency, Hz	688	608	736	576	800	624
			WDF			
β	13	11	11	12	15	12
Energy	2.98	2.83	0.58	9.90	3.62e-1	9.98e-1
Min	4.61e-2	7.19e-2	3.56e-3	3.01e-1	1.72e-3	6.30e-3
Max	1.38	0.61	3.64e-1	2.35	2.42e-1	8.61e-1
			Statistics			
$E(C_1)$	1.97e-1	1.14e-1	2.93e-2	5.01e-1	1.97e-2	5.01e-2
$Var(C_1)$	8.76e-4	3.54e-4	2.17e-5	8.92e-3	1.25e-5	1.02e-4
$V_1\delta$	26.4%	16.1%	20.2%	20.2%	21.7%	20.08%
ζ	0.0694	0.0695	0.0353	0.0372	0.0332	0.0260
			μ-*Stability*			
$[\mu_d, \mu_u]$	[6, 20]	[16, 60]	[45, 100]	[4, 12]	[80, 180]	[30, 70]
α_d	−0.0575	−0.0226	−0.0281	−0.0360	−0.0163	−0.0211
Std. Error.	5.48*e*-4	2.84*e*-4	1.99*e*-4	2.36*e*-4	1.45*e*-3	1.81*e*-4
α_u	0.0387	0.0142	0.0211	0.0282	0.0143	0.0149
Std. Error.	2.31*e*-4	8.56*e*-5	8.32*e*-5	8.43*e*-05	5.54*e*-05	6.95*e*-05

[a]Here $10^{-\beta}$ is the scale factor used for the integration kernel. The Power, Min, and Max are the energy, the minimum, and the maximum of the WDF, respectively. For each point we have the results of the stability analysis: the expectation and the variance of C_1, the relative energy error V_1^{δ}, and the factor ζ between the WDF and the expectation of C_∞. The value of $[\mu_d, \mu_u]$ used for the S index computation, and the results of linear regression α_d, α_u with their associated standard errors, are given at the bottom.

hemisphere (downgoing waves). However, there is also another peak in the opposite direction (southern hemisphere) although of much lower power.

[41] For point 2, the plane wave analysis [*Santolík and Parrot*, 2000] gives a nearly field-aligned downward propagation, with a low degree of polarization. The ERA predicts a very broad peak in the downgoing direction, at $\theta \approx 33°$, $\phi \approx 63°$. This peak fits well the primary peak of the other methods. However, in the GP and ME solutions, a secondary peak, well defined in the GP and quite questionable in the ME solution, is observed in the southern hemisphere. In the ERA, no such peak is predicted, but at most an increase of the energy occurs almost at the same place ($90° \leq \theta \leq 140°$, $30° \leq \phi \leq 120°$). Let us note that the

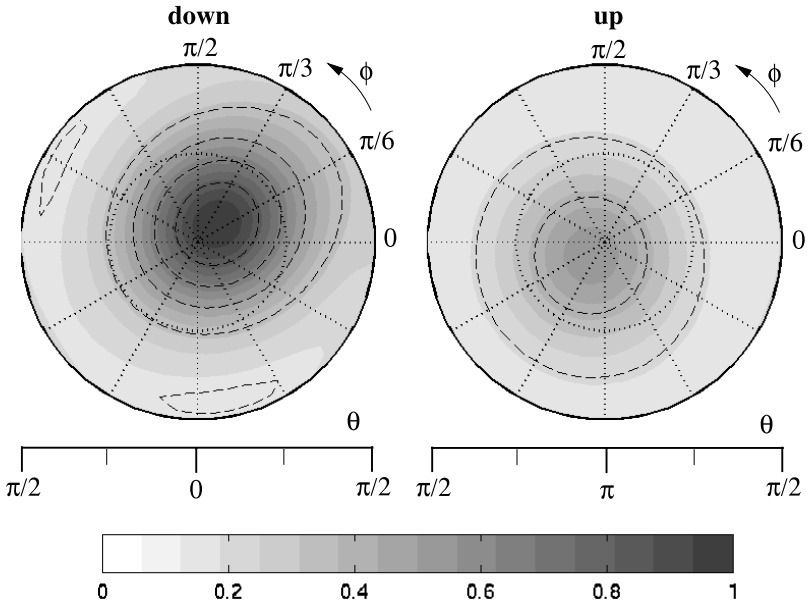

Figure 2. Example of WDF graphical representation. Here θ is the polar angle and ϕ is the azimuthal angle. The left hemisphere is for downgoing waves and the other is for upgoing ones. Contours are shown with the dashed line, which correspond to the values of {1/6, 2/6, …, 5/6}. This example shows the obtained WDF for point 1 with $\mu = 20$.

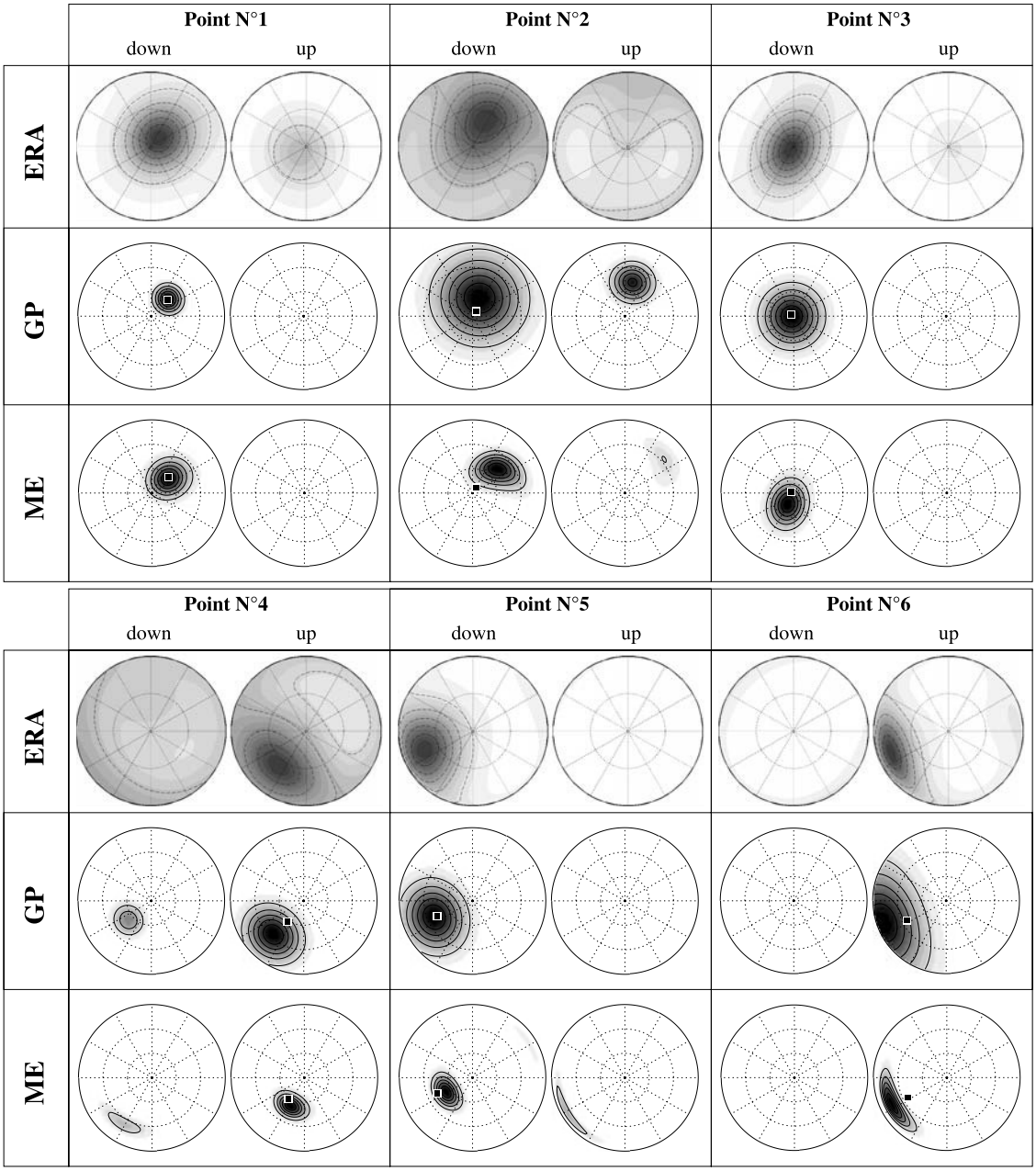

Figure 3. Results obtained by ERA (top) for the six spectral matrices. The graphical representation is similar to that in the work of *Santolík* [1995]. The wave-energy density is coded as in Figure 2. The WDF computed by the Maximum Entropy (bottom) and Gaussian Peaks (middle) methods for the points 1, 2, and 4. Borrowed from *Santolík and Parrot* [2000].

ERA solution reflects the low degree of polarization found in the plane-wave analysis [Santolik and Parrot, 2000], which means that the associated electromagnetic wave is supposed to propagate in many directions.

[42] Point 3 turns out to be quite similar to point 1, and the results obtained by the three methods confirm this similarity. Again, a secondary peak is only seen in the ERA solution in the opposite direction of the main peak. Point 4 looks like point 2, where the downgoing and upgoing waves play symmetrical roles. In other words, the main peak is observed in the southern hemisphere for point 4, while it is in the northern hemisphere for point 2.

[43] For points 5 and 6, a main peak is predicted by the three methods ($\theta \approx 60°$, $\phi \approx 201°$ for point 5, and $\theta \approx 108°$, $\phi \approx 200°$ for point 6, from the ERA solutions). There are no major discrepancies among the results obtained from the ERA, GP, and ME techniques.

4.2. Stability Analysis

[44] The results of stability test described in section 2.4 are as follows. The 1000 computations of perturbed solutions for all the six spectral matrices corresponding to the six points have been done in order to get a significant sample without excessive computation time. It took about 1

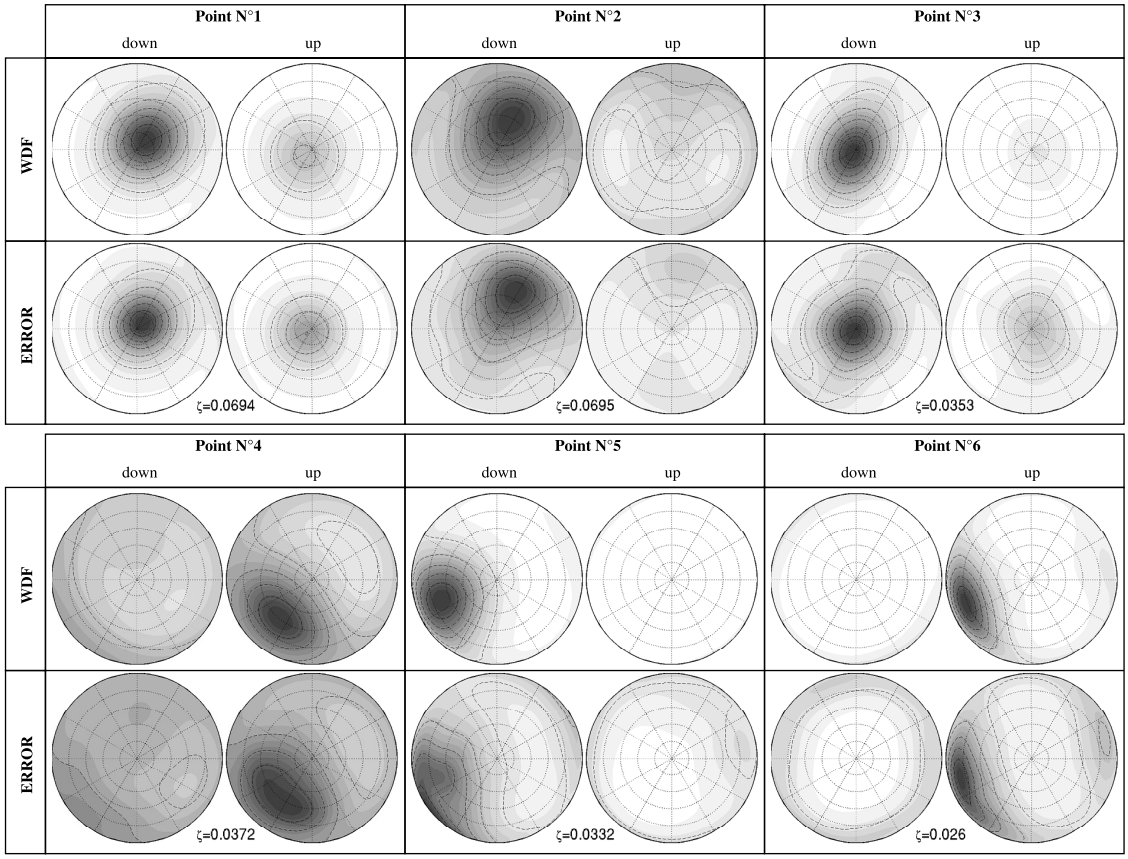

Figure 4. Results of the stability analysis. For each point the plots show the WDF and the local error, which is the expectation of C_∞. The scale factor between the WDF and the ERROR is given by the number ζ.

hour of computation for each point. In order to have perturbations of the same order as the noise level, which is about $\delta = 16$ according to the data normalization (see section 3), the variance of the Gaussian vector b has been fixed such that $E(\|V - V_N\|) = E(\|bb^*\|) \approx 10$. Nevertheless, as the variance is quite large, perturbations of the order of 60 instead of 10 are often observed.

[45] For all of the six points, an averaged energy perturbation $V_1(\delta)$ of about 21% is observed (see Table 1), which is a good result. The least energy perturbation is observed for point 2, whereas the most intense energy perturbation arises for point 1. The plots of the expectation of C_∞ for each of the six points are given in Figure 4. In this figure, the WDF and the expectation of C_∞, called ERROR, are plotted using the usual spherical representation. In addition, the scale factor ζ between the WDF and the ERROR is given in each of the six panels corresponding to the six analyzed points. The ζ values are also given in Table 1.

[46] As seen in Figure 4 as well as in Table 1, the local stability of the solutions is quite acceptable (ζ less than 7%) and the ERROR increases with the WDF value. As shown in Table 1, the highest value of $V_1(\delta)$ is the one for point 1. As 26% is not a high value, the solution remains stable. This is confirmed by choosing a higher value of μ and looking at the solution. Figure 2 shows the WDF for point 1 for a doubled value of μ. The peak is again at the same place and, as expected, the solution does not differ significantly from the one in Figure 3 (top left panel).

[47] To study the stability of the computed WDF with respect to the regularization parameter, the S index defined by (10) is computed, versus the error in the data, for each of the six points. The results are displayed in Figure 5. As can be seen, the S index decreases, almost linearly, as the error in the data increases whenever the error in the data is lower than δ, then the S index increases (again almost linearly) with the error in the data beyond δ. The slopes α_d and α_u of the decreasing and increasing parts, respectively, computed by linear regression, and their associated standard errors are given in Table 1. The largest S index is for point 1, while the lowest is for point 5. It means that the WDF is much more stable with respect to μ for point 5 than for point 1. It is worth noting that for all the points $|\alpha_d| > |\alpha_u|$ so that the greater the μ values are the better the stability is. It turns out that the stability of the ERA solution is quite high, the stability index S is indeed lower (or much lower) than 0.2 for an error in the data of $\delta - 20\%$.

5. Discussion and Conclusions

[48] In a previous paper [*Prot et al.*, 2005], a new inversion procedure was proposed to determine the wave energy density of electromagnetic fields. The wave distribution function, WDF, a concept introduced 30 years ago by

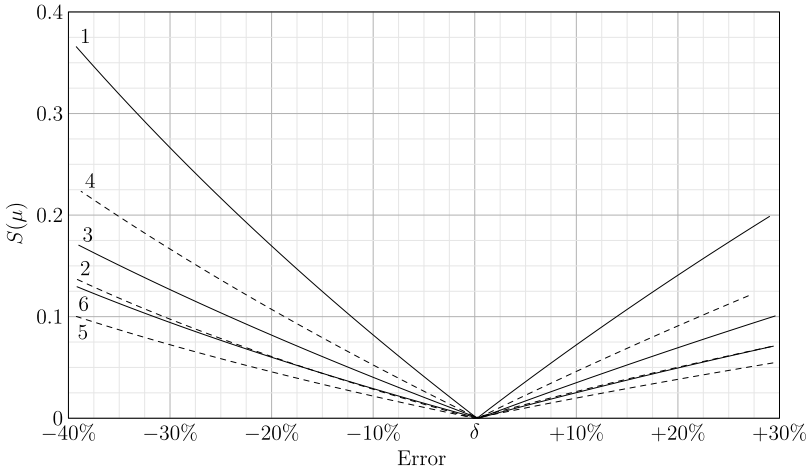

Figure 5. Analyses of solution dependences on the regularization parameter. The *S* stability index is plotted versus the error in the data for each of the six points. The curves are labelled with reference to the point number. The curves of points 1, 3, and 6 are shown as plain lines, whereas they are in dashed lines for points 2, 4, and 6.

Storey and Lefeuvre [1974] was chosen due to its ability to handle continuum plane-wave distributions. The WDF determination from field measurements implies that a highly indeterminate and ill-posed problem has to be solved. Several inversion techniques have been developed in the past, but very few of them may be applied generally. Often, some parameters have to be chosen quite arbitrarily and some a priori information has to be introduced. The entropy regularization algorithm, ERA, was therefore developed to overcome some of these limitations. In this paper the ERA has been applied to the FREJA F4 experiment electromagnetic field measurements and the results compared with those produced by two other techniques, the maximum entropy, ME, and the Gaussian peak, GP, already published in the work of *Santolík and Parrot* [2000].

[49] Overall, there is no contradiction between the ERA solutions and those computed by *Santolík and Parrot* [2000]. Globally, ERA solutions are more spread out which is expected for entropy maximization procedures. This is indeed compatible with the idea of a solution with minimal information. Let us also note that a solution with high variations (a very sharp peak) and thus large information is in contradiction with a problem which is, originally, highly indeterminate.

[50] As shown in Figure 3, for points 2 and 4, the ERA solutions exhibit a fairly constant energy in all directions, while with the two other methods, two better defined and stronger peaks are found. According to *Santolík and Parrot* [2000], the polarization degree is rather low, which is in favor of the ERA solution. Moreover, in the GP method, the a priori existence of two peaks has been imposed, which implies a lower entropy of the solution than the one for the ERA. This is also the case for the ME method. Although the existence of two peaks is not imposed in the ME, the entropy increase is due to the fact that the entropy minimization is done with a higher level of constraints than for the ERA.

[51] From this we conclude that the ME and GP solutions, which appear to be more accurate, cannot be considered as better solutions than the ERA without any extra information about the shape of the wave energy-density. This is because the ERA maximizes the entropy and therefore minimizes the information content in the solution. We should also note that the secondary peak that is observed in the GP and, to a lesser degree, in the ME methods is also detected by the ERA as an increase of the energy density. The total energy of this wave is of the same order as the one given by the ME and GP, the only difference with the ERA solution is that its energy density appears as more concentrated.

[52] At this stage of the discussion, it is worth noting that in regularization theories, a family of operators with a free parameter, $\mu > 0$, is used. For a small μ the solution produced has a small error of fit but is highly unstable. Conversely with a larger μ, the solution will deviate from the original data, but its stability will be ensured. In other words, a compromise has to be found between the error of fit and stability, by selecting a suitable value of μ. This is done automatically in the ERA, according to the Morozov's discrepancy principle, which merely requires that a solution whose error of fit is smaller than the noise level has to be rejected. As a consequence, it is always possible to choose μ values lower than the one given by the Morozov's principle in order to get solutions quite similar to the ones given by the GP and the ME techniques, knowing that their stability will be worse.

[53] When using the Morozov's discrepancy principle, it is necessary to know an approximate value δ of the noise level. A data-driven criterion could instead be used to choose μ, as in the well-known Generalized Cross Validation criterion (GCV) [*Whaba*, 1980] or the L-curve [*Hansen*, 1992]. The GCV principle is to compute the ERA solutions $F_\mu^{(i)}$ from the data vector $V^{(i)}$, which is obtained by deleting the *i*th entry of *V*. Of course the *i*th entry of the kernel *Q* is also deleted for the inversion. Then μ is chosen as the minimizer of

$$\sum_{i=1}^{16} \left(V_i - \int_0^{\pi} \int_0^{2\pi} Q_i(\theta,\phi) F_\mu^{(i)}(\theta,\phi) \sin\theta \mathrm{d}\phi \mathrm{d}\theta \right)^2 \omega_i^2 \qquad (11)$$

with weights ω_i. A simplified version of equation (11) derived by *Amato and Hughes* [1991] in entropy regularization case have been used for the computations. This criterion fails to determine the regularization parameter μ on all of the six points. The minimum of (11) is indeed obtained for a very small value of μ (such that $\varepsilon_r(V, F_\mu) < 1$). If we take a little larger value of μ, for example a μ such that $\varepsilon_r(V, F_\mu) \approx 2$, the obtained solution becomes fully instable: $E(C_1) \gg 1$. Therefore this criterion does not provide a suitable μ for the six points that are considered. In the case of classical Tikhonov's regularization, the L-curve criterion consists in drawing, for $\mu > 0$, the log-log plot of the error $\varepsilon_r(V, F_\mu)$ versus the norm of F_μ. This plot is L-shaped and μ is chosen as the point of maximum curvature of the curve: the corner of the L. This criterion also fails to provide a suitable μ: the observed curve of the error $\varepsilon_r(V, F_\mu)$ versus the entropy $H(F_\mu)$ is not L-shaped, it is convex and decreases with a quasi-constant curvature. In fact, the curvature increases as μ decreases; therefore this criterion leads also to a very small value of μ, which is not suitable. The instability of the solution for such a μ value is indeed dramatic. The GCV and L-curve criterions are well-known methods for choosing the regularization parameter; however, these criterions seems to not apply for the ERA method. On the other hand, the small number of available data vectors ($V \in \mathbb{C}^n$) may also explain the poor performance of these methods. The development of a data-driven method for choosing μ actually stays an open problem.

[54] Although the stability of the solutions obtained to fit the FREJA data is controlled by the ERA algorithm, a statistical study has been performed to quantify it as a whole and point by point. To do this, the spectral matrices have been perturbed and the resulting energy deviation and the variation for each points of the WDF have been estimated. On the average, and for the six events considered in this study, the energy deviation turns out to be near 20%, while the variation for each points of the WDF is less than 7%. The stability of the solution with respect to the parameter μ have been analyzed, and the results have shown the stability of the computed ERA solutions. It is quite clear that an increase of stability with respect to the regularization parameter is theoretically expected, since for large μ values the solution only depends on the penalty function. This increase of stability is shown in Table 1, by the dissymmetry of the slope of the S index for all of the six points.

[55] As a final conclusion, we have shown that the entropy regularization algorithm, ERA, is well suited to analyze wave characteristics in space plasmas. It allows the wave distribution function, WDF, to be computed and, in particular, the wave propagation direction to be determined. Unlike other methods, such as the maximum entropy, ME, and Gaussian peaks, GP, the ERA does not need any assumptions, for example, about the shape of the WDF and/or the significance of the integration kernels. Therefore a good strategy in analyzing a large amount of data is first to apply the ERA to detect the wave events we are interested in and then to use other techniques, for example the GP and/or ME, to refine the diagnostics of these waves. Alternatively, the ERA can also be used in the diagnostics refinement step by choosing the appropriate value of the regularization parameter μ.

[56] **Acknowledgments.** The authors wish to thank M. Bergounioux (CNRS-MAPMO, Orléans, FRANCE), J. L. Pinçon, and F. Lefeuvre (CNRS-LPCE, Orléans, FRANCE) for their very helpful suggestions. O. Santolík acknowledges additional support from ESA PECS contract 98025. Many thanks for the valuable referee's comments.

[57] Arthur Richmond thanks the reviewers for their assistance in evaluating this paper.

References

Amato, U., and W. Hughes (1991), Maximum entropy regularization of Fredholm integral equations of the first kind, *Inverse Problems*, *7*, 739–808.

Bergounioux, M. (2002), *Optimisation et Controle des Systémes Linéaires*, Dunod, Paris.

Engl, H. W., and G. Landl (1993), Convergence rates for maximum entropy regularization, *SIAM J. Numer. Anal.*, *30*, 1509–1536.

Hansen, P. C. (1992), Analysis of discrete ill-posed problems by means of the *L*-curve, *SIAM Rev.*, *34*, 561–580.

Holback, B., S. E. Jansson, L. Ahlen, G. Lundgren, L. Lyngdal, S. Powell, and A. Meyer (1994), The FREJA wave and plasma density experiment, *Space Sci. Rev.*, *70*, 577–592.

Kirsch, A. (1996), *An Introduction to the Mathematical Theory of Inverse Problems*, Springer, New York.

Lefeuvre, F. (1977), Analyse de champs d'ondes Électromagnétiques aléatoires observées dans la magnétosphére partir de la mesure simultanée de leur six composantes, Thése d'état, Univ, d'Orléans, Orléans, France.

Lefeuvre, F., and C. Delannoy (1979), Analysis of random electromagnetic wave field by a maximum entropy method, *Ann. Telecom.*, *34*, 204–213.

Lefeuvre, F., and C. Delannoy (1986), A computer program for the maximum entropy estimation of wave distribution function, *Comput. Phy. Comm.*, *40*, 389–419.

Lefeuvre, F., and J. L. Pinçon (1992), Determination of the wave-vector spectrum for plasma waves and turbulence observed in space plasmas, *J. Atmos. Terr. Phys.*, *54*, 1227–1235.

Lefeuvre, M., F. Parrot, and C. Delannoy (1981), Wave distribution function estimation of VLF electromagnetic waves observed on board GEOS 1, *J. Geophys. Res.*, *86*, 2359–2375.

Oscarsson, T. (1994), Dual principles in maximum entropy reconstruction of the wave distribution function, *J. Comput. Phys.*, *110*, 221–233.

Oscarsson, T., G. Stenberg, and O. Santolik (2001), Wave mode identification via wave distribution function analysis, *Phys. Chem. Earth*, *26*, 229–235.

Press, W., S. Teutolsky, W. Vetterling, and B. Flannery (1986), *Numerical Recipes*, Cambridge Univ. Press, New York.

Prot, O., O. Santolik, and J. Trotignon (2004), Ill-posed problem solving by an entropy regularization method: Application to the propagation analysis of electromagnetic waves, in *WDS'04 Proceedings of Contributed Papers: Part III - Physics*, edited by J. Safrankova, pp. 593–599, Matfyzpress, Prague.

Prot, O., M. Bergounioux, and J. G. Trotignon (2005), Determination of a power density by an entropy regularization method, *J. Appl. Math.*, *2*, 127–152.

Santolík, O. (1995), Etude de la fonction de distribution des ondes dans un plasma chaud, Thése, Univ. d'Orléans, Orléans, France.

Santolík, O., and M. Parrot (1996), The wave distribution function in a hot magnetospheric plasma: The direct problem, *J. Geophys. Res.*, *101*, 10,639–10,651.

Santolík, O., and M. Parrot (2000), Application of wave distribution function methods to an ELF hiss event at high latitudes, *J. Geophys. Res.*, *105*, 18,885–18,894.

Shore, J. E., and R. W. Johnson (1980), Axiomatic derivation of the principle of maximum entropy and the principle of minimum cross-entropy, *IEEE Trans. Inf. Theory*, *26*, 26–36.

Smith, C., and W. J. Grandy (1987), *Maximum-Entropy and Bayesian Spectral Analysis and Estimations Problems*, Springer, New York.

Styx, T. (1992), *Waves in Plasmas*, Am. Inst. of Phys., New York.

Storey, L. (1987), Wave distribution function analysis of plasmaspheric hiss, *Tech. Rep. D-711-2*, STAR Lab., Stanford Univ., Stanford, Calif.

Storey, L. R. O., and F. Lefeuvre (1974), Theory for the interpretation of measurements of a random electromagnetic wave field in space, *Space Res.*, *14*, 381–386.

Storey, L. R. O., and F. Lefeuvre (1979), The analysis of 6-component measurement of a random electromagnetic wave field in a magnetoplasma: 1. The direct problem, *Geophys. J. R. Astron. Soc.*, *56*, 255–270.

Storey, L. R. O., and F. Lefeuvre (1980), The analysis of 6-component measurement of a random electromagnetic wave field in a magnetoplasma: 2. The integration kernels, *Geophys. J. R. Astron. Soc.*, *62*, 173–194.

Tikhonov, A., and V. Arsenin (1977), *Solutions of Ill-Posed Problems*, John Wiley, Hoboken, N. J.

Tikhonov, A. N., A. V. Goncharsky, V. Stepanov, and A. Yagola (1995), *Numerical Methods for the Solution of Ill-Posed Problems*, Springer, New York.

Whaba, G. (1980), Ill-posed problems: Numerical and statistical method for mildly, moderately and severely ill posed problems with noisy data, *Tech. Rep. 595*, Univ. of Wisconsin, Madison, Wisc.

H. Deferaudy, Centre d'Étude des Environnements Terrestre et Planétaires, Institut Pierre Simon Laplace, 10-12 Rue de l'Europe, F-78140 Vélizy, France. (herve.deferaudy@cetp.ipsl.fr)

O. Prot, Laboratoire MIP, Université Paul Sabatier, F-31062 Toulouse Cedex 9, France. (oprot@mip.ups-tlse.fr)

O. Santolík, Faculty of Mathematics and Physics, Charles University, V Holesovickach 2, CZ-18000 Prague 8, Czech Republic. (ondrej.santolik@mff.cuni.cz)

J.-G. Trotignon, Laboratoire de Physique et Chimie de l'Environnement, Centre National de la Recherche Scientifique, 3A, Avenue de la Recherche Scientifique, F-45071 Orléans Cedex 2, France. (jean-gabriel.trotignon@cnrs-orleans.fr)